Journal of Biomechanics 49 (2016) 289–294

Contents lists available at ScienceDirect

Journal of Biomechanics

journal homepage: www.elsevier.com/locate/jbiomech
www.JBiomech.com

# Simplified versus geometrically accurate models of forefoot anatomy to predict plantar pressures: A finite element study

Scott Telfer [a,b,*], Ahmet Erdemir [c], James Woodburn [b], Peter R. Cavanagh [a]

[a] Department of Orthopaedics and Sports Medicine, University of Washington, Seattle, WA, USA
[b] Institute for Applied Health Research, Glasgow Caledonian University, Glasgow G4 0BA, UK
[c] Computational Biomodeling (CoBi) Core & Department of Biomedical Engineering, Lerner Research Institute, Cleveland Clinic, Cleveland, OH, USA

ARTICLE INFO

*Article history:*
Accepted 7 December 2015

*Keywords:*
Foot
Finite element analysis
Plantar pressure
Diabetes
Insoles
Orthotics

ABSTRACT

Integration of patient-specific biomechanical measurements into the design of therapeutic footwear has been shown to improve clinical outcomes in patients with diabetic foot disease. The addition of numerical simulations intended to optimise intervention design may help to build on these advances, however at present the time and labour required to generate and run personalised models of foot anatomy restrict their routine clinical utility. In this study we developed second-generation personalised simple finite element (FE) models of the forefoot with varying geometric fidelities. Plantar pressure predictions from barefoot, shod, and shod with insole simulations using simplified models were compared to those obtained from CT-based FE models incorporating more detailed representations of bone and tissue geometry. A simplified model including representations of metatarsals based on simple geometric shapes, embedded within a contoured soft tissue block with outer geometry acquired from a 3D surface scan was found to provide pressure predictions closest to the more complex model, with mean differences of 13.3 kPa (SD 13.4), 12.52 kPa (SD 11.9) and 9.6 kPa (SD 9.3) for barefoot, shod, and insole conditions respectively. The simplified model design could be produced in $<1$ h compared to $>3$ h in the case of the more detailed model, and solved on average 24% faster. FE models of the forefoot based on simplified geometric representations of the metatarsal bones and soft tissue surface geometry from 3D surface scans may potentially provide a simulation approach with improved clinical utility, however further validity testing around a range of therapeutic footwear types is required.


## 1. Introduction

Few tools exist to provide quantitative insight into the prescription of therapeutic footwear for conditions with a high disease burden, such as diabetic foot disease. Currently, the design of these interventions tends to be derived subjectively by the attending pedorthist/orthotist based on clinical experience. It has recently been demonstrated that, when compared to devices prescribed using standard methods, the inclusion of plantar pressure measurements into the design process for footwear intended to prevent plantar ulceration in individuals with diabetes can improve offloading performance (Owings et al., 2008) and reduce ulceration rates (Bus et al., 2013; Ulbrecht et al., 2014). Similarly, plantar pressure driven design rules have been suggested for the design of foot orthoses in patients with rheumatoid arthritis (Gibson et al., 2014) and military recruits (Franklyn-Miller et al., 2011). Such studies provide evidence that objective biomechanical assessment can bring clinically relevant advantages over subjective methods for orthotic prescription.

Building on these findings, a potential technological advance that may help further optimise the design of the footwear interventions before they are delivered to the patient is the use of numerical simulation techniques such as finite element (FE) analysis. These techniques can be applied for *a priori* prediction of the mechanical response of the foot to a given footwear intervention (Telfer et al., 2014). A number of studies based on this type of approach have been published, and have provided insights into several aspects of foot biomechanics, including internal and surface stresses (Chen et al., 2010; Fontanella et al., 2014; Gefen, 2003), blood supply to soft tissues (Mithraratne et al., 2012) and therapeutic footwear design (Actis et al., 2008; Chen et al., 2015; Cheung and Zhang, 2005). While informative, most of these studies used FE models of the foot that were not constructed with

* Corresponding author at: Institute for Applied Health Research, Glasgow Caledonian University, Glasgow G4 0BA, UK. Tel.: +44 0 141 331 8475.
*E-mail address:* scott.telfer@gcu.ac.uk (S. Telfer).

http://dx.doi.org/10.1016/j.jbiomech.2015.12.001
0021-9290/

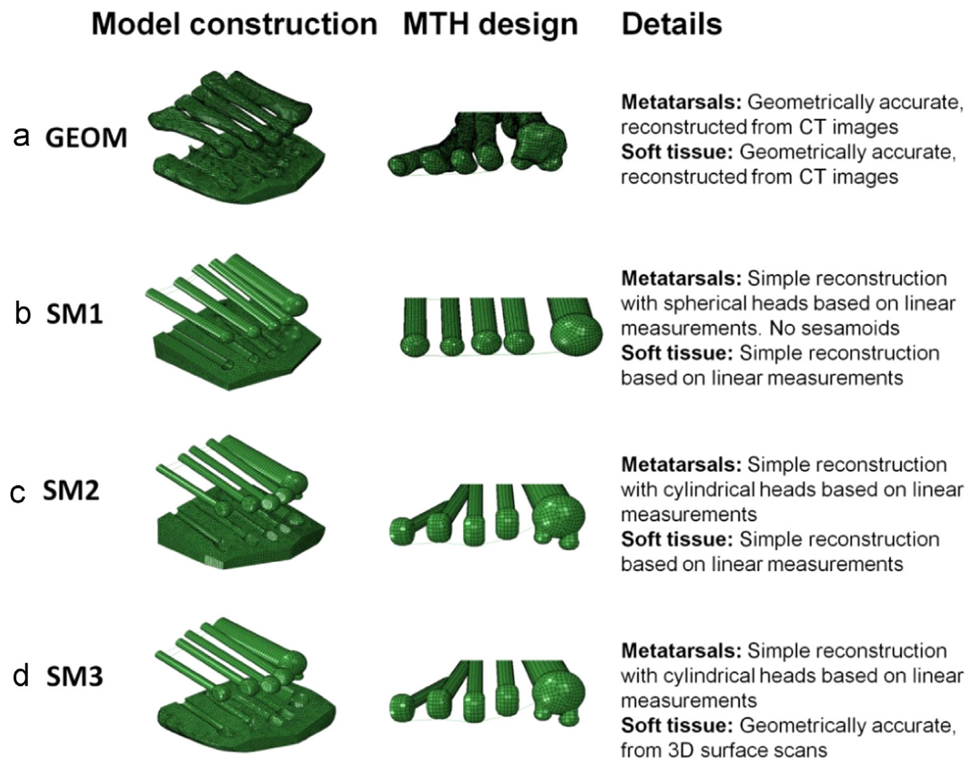


**Fig. 1.** Model designs: (a) GEOM; (b) SM1; (c) SM2; (d) SM3 with construction overview and design details. See Supplementary material for further details. Please note MTH orientation in each model and accommodation of tissue thickness.

routine clinical utility in mind and required considerable time and effort to build and run.

A personalised, clinically useful FE model should be fast to construct and solve, and must be adequate in terms of predicting the biomechanical variables of interest, particularly when simulating the effects of interventions. Currently, the most commonly used workflow to produce a personalised foot model requires reconstruction of bone and soft tissue anatomy in full from computed tomography (CT) and/or magnetic resonance (MR) imaging data. This is a time consuming and expensive process requiring a considerable amount of expert user interaction.

We previously presented a simplified FE model of the forefoot based on geometrically simplified shapes to represent both the metatarsals and bulk soft tissues (Spirka et al., 2014). This demonstrated the feasibility of generating a fast to build and solve model that could potentially inform clinical decision making with regards to the prescription of footwear design. The aim of the present study is to investigate the effects of altering the level of geometric fidelity of forefoot models used to predict plantar pressures under the metatarsal heads. In addition, model development times and simulation costs were investigated to evaluate model feasibility for routine clinical use.

## 2. Methods

### 2.1. Data collection

Eight healthy volunteers, 4♀, age 38.2 years (SD 10.0), height 1.71 m (SD 0.11), weight 70.3 kg (SD 10.6) were recruited for this study. Ethical approval was obtained from the local Institutional Review Board (ref: 10/S1001/24) and participants gave informed, written consent. CT scans of the unloaded right foot from all participants were obtained using an effective slice thickness of 1 mm in the axial plane and an in-plane resolution of 0.6 mm (Oosterwaal et al., 2011) for the purpose of building the geometrically detailed model. Participants walked barefoot over a plantar pressure measurement platform (0.5 m Advanced footscan® System; RSScan International NV, Paal, Belgium) five times at a self-selected but consistent speed. The platform, which uses an array of 5 mm × 8 mm sensors, recorded contact pressures at 500 Hz and was mounted on top of a force plate (Type 9286B; Kistler Instrument Corp, Amherst, NY) to allow dynamic calibration. Three-dimensional surface scans of the right foot were taken with the foot unloaded using a laser scanner (Easy Foot Scan; OrthoBaltic Kaunas, Lithuania). The data were divided into two sets: a training set (5 participants) which was used to optimise the design of the simple FE models; and a validation set (3 participants) which was used to assess the external validity of the best performing model design.

### 2.2. Data processing

Metatarsal and soft tissue geometries were manually segmented from the CT data using Scan IP software (V6.0; Simpleware Ltd, Exeter, UK). These were used in the model with full geometric detail. To achieve the aim of having a simplified model design that is fast to build, bone geometry had to be represented by simple geometric shapes. These shapes should be produced and assembled in an automated manner based on easily obtainable measurements from ultrasound images of the anatomy, as this is a low-cost and accessible measurement technique compared to CT or MRI. Therefore a series of linear and angular measurements were taken from the imaging data including metatarsal head (MTH) diameters, plantar soft tissue thickness under each MTH, and the relative position of each metatarsal. A full description of the measurements obtained and how they were used as inputs to the different FE model designs is provided in the Supplementary materials. Processing of segmented files, surface scans and production of simplified bone geometries were carried out using FreeCAD (V0.13; www.freecadweb.org). Mean plantar pressures under the individual MTHs at the instance of peak forefoot force were averaged across all five walking trials for each participant.

### 2.3. Model design

All models were assembled and run in the finite element analysis package Abaqus (V6.10; Simulia, Providence, RI) using the implicit static solver. The basic form of the forefoot in each model design consisted of a bulk soft tissue component, the metatarsal bones, and inter-metatarsal ligaments. The soft tissue was modelled as a lumped nearly-incompressible Ogden hyperelastic material, $\mu$=0.0375 MPa, $\alpha$=5.5, effective Poisson's ratio=0.49 (Chen et al., 2012). To reduce solution times, the dorsal soft tissue above the midline of the metatarsals was removed using Boolean subtraction (see Fig. 1). Individual metatarsal bones were represented as rigid shell components; and inter-metatarsal ligaments that restrained medio-lateral splay of the bones were modelled as tension-only truss elements ($E$=260 MPa, Poisson's ratio=0.3 (Cheung and Zhang, 2008)). A total of 11 ligament locations were included based on the descriptions and drawings provided in Primal Pictures 3D Anatomy Software (Primal Pictures Limited, London, UK).

Linear tetrahedral elements (C3D4) with a characteristic element length of 1.8 mm were used for the soft tissue to ensure fast and efficient meshing. A convergence analysis demonstrated changes in plantar pressure predictions of $<5\%$ when the element length was reduced by 50%. The use of linear tetrahedral elements, although common in FE foot studies (Cheung and Zhang, 2008; Isvilanonda et al., 2012), may affect the accuracy of predictions due to shear locking (Tadepalli et al., 2011). To ensure the chosen element performed adequately, barefoot models associated with one randomly chosen participant were rerun after the standard analysis using quadratic tetrahedral elements (C3D10) which are able to compensate for this effect. The difference between the linear and quadratic models was found to be $<5$ kPa in all cases, suggesting the use of linear elements was adequate for this study.

In total, four model designs (one geometrically accurate and three simplified) were tested and are described in brief here (Fig. 1). Further information relating to their construction is provided in the Supplementary materials.

(1) **The geometrically accurate model (GEOM)**. This model design used geometrically accurate bone and soft tissue parts reconstructed directly from the participants' CT scans.
(2) **First generation Simple Model (SM1)**. This simplified model design is described in detail in Spirka et al. (2014). In short, MTHs were represented with spheres scaled to the MTH diameter with cylinders representing the metatarsal shaft. Soft tissue was modelled as a modified rectangular block with dimensions defined by the width of the forefoot and length of the metatarsals.
(3) **Second generation Simple Model with rectangular soft tissue (SM2)**. This simplified model design used a different geometric design for the MTHs of the lesser metatarsals compared to the SM1 model. These MTHs were modelled as a cylinder with its width and diameter defined by the width of the MTH geometry and a circle fitted to the sagittal plane view of the MTH respectively. Fillets were applied to the edges of the cylinder based on a standardised rule. The MTH1 sesamoids, which were not part of the SM1 model, were added as cylinders with hemispherical ends. The angle of the metatarsals in the coronal plane was also taken into account in the SM2 model. The soft tissue was again modelled as a modified rectangular block defined by the dimensions of the forefoot anatomy.
(4) **Second generation Simple Model with patient-specifc soft tissue geometry (SM3)**. This simplified model used the same metatarsal design and placement described in SM2. However, rather than using a geometric approximation of the surface of the soft tissue, the SM3 model was based on the true plantar shape of each patient's forefoot obtained from an unloaded 3D surface scan, which was trimmed anteriorly and posteriorly to the required dimensions.

For each of the four model designs, a simulation of peak loading during the barefoot walking condition was produced where the forefoot model was placed in contact with an analytically rigid component representing the floor. Surface-to-surface contact interactions were defined between the floor and the soft tissue, and in all cases a static coefficient of friction of 0.5 was used.

If the model was able to simulate regional contact pressures that were on average within 25 kPa (a value judged by the authors to be the maximum acceptable error based on a review of the literature (Telfer et al., 2014)) of those given under the MTHs by the GEOM model design, two further scenarios were tested; a shod condition where a component of dimensions $130 \times 130 \times 10\ \text{mm}^3$ representing the shoe was introduced between the foot and the floor; and a shoe plus insole condition where an additional component representing a flat insole (dimensions $130 \times 130 \times 6\ \text{mm}^3$) was placed between the forefoot and the shoe component. The footwear components were modelled in a similar manner to those described in Spirka et al. (2014), with a 10 mm layer of Firm Crepe (modelled as a hyperfoam material; $\mu=1.086$ MPa, $\alpha=27.62$, $\beta=0.091$) representing the shoe, meshed using C3D8 hexahedral elements with characteristic length of 3.3 mm. A 6 mm layer of Plastazote® Medium (hyperfoam; $\mu=0.488$, $\alpha=26.09$, $\beta=0.07$) represented the insole, again meshed using C3D8 hexahedral elements with characteristic length of 2 mm. Material properties were taken from Petre et al. (2006). Surface-to-surface contact interactions (coefficient of friction$=0.5$) were defined between the top surface of the shoe component and the soft tissue, and the top surface of the insole component and the soft tissue for the shod and insole conditions respectively. In the footwear simulations, the lower surface of the shoe was tied to the floor and the lower surface of the insole was tied to the upper surface of the shoe as required.

For the GEOM models, concentrated point loads were applied to the most inferior point of each of the MTHs and loads were adjusted until the predicted pressure under each MTH matched that of the experimentally measured distribution to within 5 kPa (as described in Spirka et al. (2014)) in a subject-specific manner. These loads, derived from the barefoot condition, were then used for all of the simulations using the simplified model designs across all of the simulation conditions, barefoot and footwear-based.

After the initial model runs on the training dataset, the best-performing simplified model design was used to produce personalised models based on the data for the three participants in the validation dataset for all test conditions. This additional analysis was carried out in order to check the external validity of the design as the training dataset was used to optimise the design algorithms for the simplified models during the development stages.

### 2.4. Analysis

All statistical analyses were performed using R version 3.1.1 (R Development Core Team, 2014) and figures presenting data were produced using the ggplot2 package (Wickham, 2009). The predicted peak mean pressure across a mask on the plantar surface of the soft tissue component below each MTH was used as the primary basis for comparisons between models. Absolute differences between the GEOM and simplified models were compared using a repeated measures analysis of variance ($\alpha=0.05$) followed by post-hoc pairwise $t$-tests (adjusted for multiple comparisons).

The wall-clock time taken to solve the model designs were compared between models using Kruskal–Wallis analysis of variance followed by Wilcoxon signed-rank tests. Analysis of build times was limited to the GEOM models and the best performing simplified model across the validation dataset (3 individuals) to minimise any learning effects that may have occurred during the development phase. These variables were analysed using descriptive statistics.

Model simulations were run on 8 cores (Intel Xeon E5405 CPUs, 2 GHz). To obtain estimates for the potential improvements in performance of the best performing simplified model design on higher-specification computing equipment, the run time was obtained for a randomly chosen model (insole condition) on a system with 8 Intel Xeon E5-2680 CPUs (2.2 GHz) and an Nvidia K20m GPU.

## 3. Results

Exemplar predicted pressure distributions for models associated with a single participant are shown in Fig. 2. Similar plots for all participants are provided in the Supplementary materials. Summary results for differences between the simplified and the GEOM models are given in Fig. 3. The best performing simplified model design was found to be the SM3 design, which for the training set gave mean differences of 13.3 kPa (SD 13.4), 12.52 kPa (SD 11.9) and 9.6 kPa (SD 9.3) for barefoot, shod and insole conditions respectively when compared to the GEOM model across all 5 MTH regions in all subjects. These results were significantly better than the SM2 design in the shod ($p=0.017$, 95% CI [1.12, 10.32]) and insole ($p=0.009$ 95% CI [1.33, 8.42]) conditions, although there were no statistically significant differences for the barefoot conditions ($F(2,8)=3.144$, $p=0.098$). The SM1 model did not achieve the preselected cut off of an average difference of $<25$ kPa for the barefoot simulations so was not tested in the footwear conditions. The absolute differences for the validation dataset in terms of plantar surface pressure predictions from the SM3 model design compared to the GEOM were similar to those found in the training set, with mean errors of 12.8 kPa, 10.2 kPa and 8.5 kPa for barefoot, shod and insole respectively. The range fell within that seen for the training dataset, supporting the external validity of the simplified SM3 model design.

Analysis of variance revealed model run times to be significantly different in the barefoot condition ($p=0.01742$, $H=10.1$) but not within the shod ($p=0.068$, $H=5.4$) or insole ($p=0.095$, $H=4.7$) conditions (see Fig. 4). Post hoc testing of the barefoot condition revealed significant pairwise differences between the GEOM and SM3 models ($p=0.004$, $V=0$), and the GEOM and SM2 models ($p=0.003$, $W=2$) with the simplified models solving faster. Mean build times for the GEOM and SM3 models were 194 min (range 161–228) and 54 min (range 48–58) respectively. The mean mesh size for the anatomical components was 36809 elements for the GEOM model, and 29453, 26862 and 28743 for SM1, SM2 and SM3 respectively.

Using a higher performance system to rerun a randomly selected insole model reduced the run time by a factor of $\sim 3$, from 93 min to 31 min.

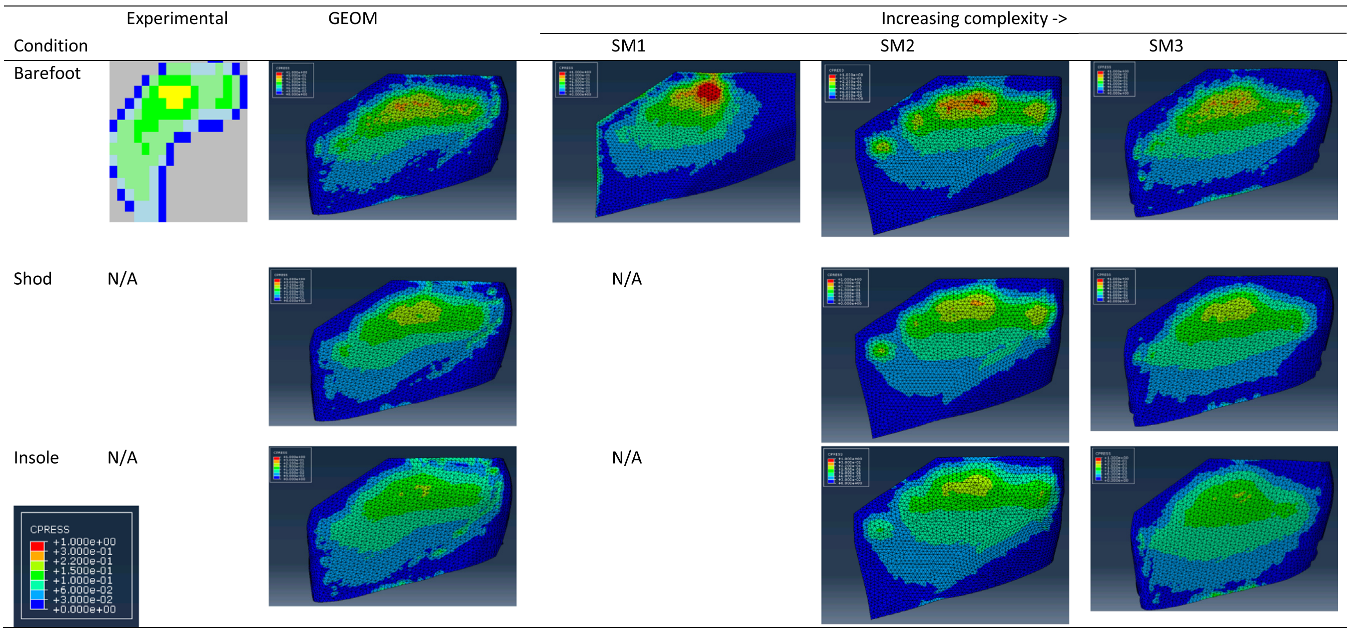


**Fig. 2.** Predicted pressure distributions from all models and conditions for a single participant. Simplified models are presented as increasing in fidelity left to right. Individual images are oriented with distal (top) to proximal (bottom), and lateral (left) to medial (right). See Supplementary material for other examples. Note that a representative image, mirrored for ease of comparison, is used for experimental and data used for models is mean of several trials. Data are in MPa.

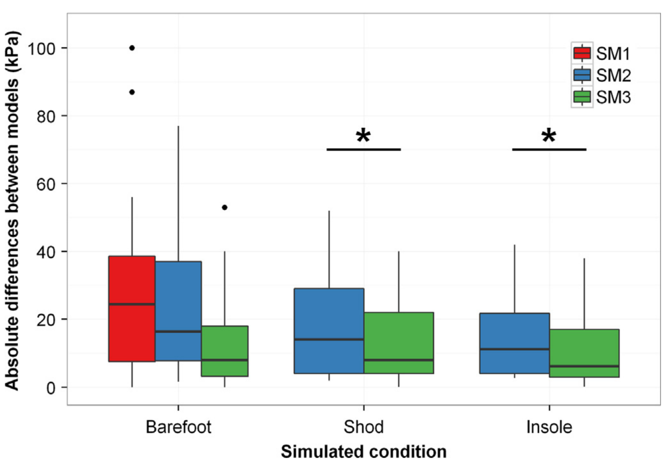


**Fig. 3.** Differences in pressure predictions for each model averaged across MTHs and participants are presented as boxplots. The box signifies the upper and lower quartiles, and the mean is represented by the black line within the box. Outliers are represented as individual points. Statistically significant differences between models are indicated with "*".

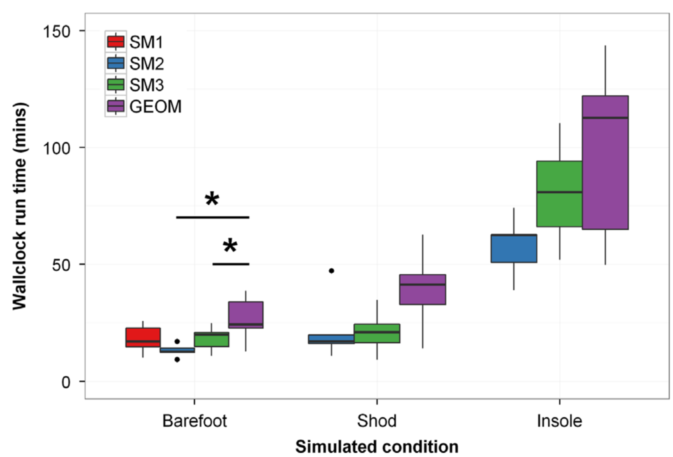


**Fig. 4.** Simulation times for models of different fidelities are presented as boxplots. The box signifies the upper and lower quartiles, and the mean is represented by the black line within the box. Outliers are represented as individual points. Statistically significant differences between models are indicated with "*".

## 4. Discussion

A key factor in producing simplified models with direct patient utility is identifying the minimum dataset required to produce a clinically useful model of the forefoot. The best performing model here (SM3 design) required estimates of plantar tissue thickness, MTH morphology, and full soft tissue surface geometry. The redesign of the MTHs in the SM2 and SM3 models showed a trend towards improved predictions compared to the SM1 model. We believe a considerable error component in the SM1 model resulted from the lack of a specific representation of the sesamoids – which were included in the second generation models. The inclusion of accurate soft tissue plantar surface geometry obtained via the unloaded 3D surface scans did further improve the model predictions, suggesting that an accurate representation of this anatomy is necessary for a simplified model to produce a better match with the experimental data.

All measurements required to produce the simplified models presented in this paper can be obtained using more accessible clinical tools and assessments, including ultrasound and 3D surface scanning. Ultrasound is an appealing alternative to CT or MRI (commonly used in foot modelling studies (Chen et al., 2014; Cheung and Zhang, 2008)) as it is a low-cost and accessible measurement technique that does not involve exposure to ionising radiation. 3D surface scanners are widely available at relatively low-cost and require minimal training on the part of the operator (Telfer and Woodburn, 2010).

While statistically significant improvements were seen only for run times in the barefoot condition with the simplified compared to the GEOM models, trends towards differences in the footwear conditions were seen, and a larger sample size is likely to show these as statistically significant. Our results demonstrated that a further threefold reduction in runs times could be achieved using a higher performance computing hardware (including a GPU processor) compared to our standard workstation.

In addition to solution times, a key component for providing a clinically useful FE model is the build time. The SM3 model design took approximately one third of the time to construct compared to the GEOM model. A significant proportion of this difference was associated with segmentation of the metatarsals from the raw CT data. From our experience, a typical metatarsal bone can be segmented and exported from an image stack (1 mm spacing and orientated orthogonally to the long axis of the bone) in approximately 15 min including importing and exporting of the raw and processed data using commercially available software. Performing the equivalent operation for MRI images can take significantly longer.

A further advantage of simplifying the bone geometries is parametrisation. This can allow quick generation of models that can be incorporated into unsupervised iterative analyses. Construction of the components for the simple models for this study was partially automated using the scripting functions in the computer aided design and FE software and takes only a few minutes. Simplified bone files were also considerably faster to import into the FE analysis program than the real bone files. GEOM models also tended to require additional post-processing of meshes even using tetrahedral elements to ensure high quality mesh was obtained. Morphing template meshes has been proposed as an alternative approach (Tadepalli et al., 2011); however the high likelihood of encountering patients with significant deformities may limit the applicability of this approach.

A number of limitations and factors that require further research should be noted. The methodological nature of this study, focused on the analysis of model design, meant that we did not directly test the predictive ability of the simplified models for footwear interventions and compare them to experimentally derived measurements. Previous results using the SM1 model showed relatively poor predictive ability for therapeutic footwear featuring metatarsal pad features (Spirka et al., 2014) however this model did not use the true surface geometry of the foot. The ability of the improved simple models reported here to predict the effects of more complex, contoured footwear interventions requires further exploration and evaluation before it can be determined if they have true clinical utility.

For this study we used material properties for the lumped forefoot plantar tissues that were drawn from the literature. Demonstrated variability in these tissues means that in order for the model to provide accurate, personalised predictions of plantar pressures, the individual-specific material properties will be required as an input to the model. These tissues are known to be viscoelastic (Fontanella et al., 2014; Pai and Ledoux, 2010), and this factor was not included in our material model. However for the quasistatic simulations of walking loads this approach has been demonstrated to be adequate and has been used in a number of modelling studies (Chen et al., 2014). In addition, modelling the soft tissue as lumped material is adequate for predicting surface stresses but not internal stresses (Petre et al., 2013). Elevated shear forces have also been proposed as a potential cause of ulceration (Yavuz et al., 2007) and these were not included in the simulations.

## 5. Conclusion

This work has extended the concept of simplified personalised finite element models of the forefoot. Such models can be generated through clinic-based measurement techniques that are more accessible and less expensive than modalities such as MRI or CT, and perform well in comparison to more detailed FE models. The advantages of the simplified approach, particularly the greatly reduced build time, may improve the utility of the technique and bring it closer to clinical feasibility in terms of integration into the process of footwear and insole design.

## Conflict of interest statement

PRC has equity in DIApedia LLC and AE has equity in innodof LLC.

## Acknowledgements

ST is funded through the People Programme (Marie Skłodowska-Curie Actions) of the European Union's Seventh Framework Programme (FP7 2007–2013) under REA Grant Agreement no. PIOF-GA-2012-329133.

## Appendix A. Supplementary material

Supplementary data associated with this article can be found in the online version at http://dx.doi.org/10.1016/j.jbiomech.2015.12.001.

## References

Actis, R.L., Ventura, L.B., Lott, D.J., Smith, K.E., Commean, P.K., Hastings, M.K., Mueller, M.J., 2008. Multi-plug insole design to reduce peak plantar pressure on the diabetic foot during walking. Med. Biol. Eng. Comput. 46, 363–371.

Bus, S.A., Waaijman, R., Arts, M., de Haart, M., Busch-Westbroek, T., van Baal, J., Nollet, F., 2013. Effect of custom-made footwear on foot ulcer recurrence in diabetes: a multicenter randomized controlled trial. Diabetes Care 36, 4109–4116.

Chen, W.-M., Lee, S.-J., Lee, P.V.S., 2014. The in vivo plantar soft tissue mechanical property under the metatarsal head: implications of tissues' joint-angle dependent response in foot finite element modeling. J. Mech. Behav. Biomed. Mater. 40, 264–274.

Chen, W.-M., Lee, S.-J., Lee, P.V.S., 2015. Plantar pressure relief under the metatarsal heads – therapeutic insole design using three-dimensional finite element model of the foot. J. Biomech. 48, 659–665.

Chen, W.-M., Lee, T., Lee, P.V.-S., Lee, J.W., Lee, S.-J., 2010. Effects of internal stress concentrations in plantar soft-tissue – a preliminary three-dimensional finite element analysis. Med. Eng. Phys. 32, 324–331.

Chen, W.-M., Park, J., Park, S.-B., Shim, V.P.-W., Lee, T., 2012. Role of gastrocnemius-soleus muscle in forefoot force transmission at heel rise – a 3D finite element analysis. J. Biomech. 45, 1783–1789.

Cheung, J.T.-M., Zhang, M., 2005. A 3-dimensional finite element model of the human foot and ankle for insole design. Arch. Phys. Med. Rehabil. 86, 353–358.

Cheung, J.T.-M., Zhang, M., 2008. Parametric design of pressure-relieving foot orthosis using statistics-based finite element method. Med. Eng. Phys. 30, 269–277.

Fontanella, C.G., Favaretto, E., Carniel, E.L., Natali, A.N., 2014. Constitutive formulation and numerical analysis of the biomechanical behaviour of forefoot plantar soft tissue. Proc. Inst. Mech. Eng. H 228, 942–951.

Franklyn-Miller, A., Wilson, C., Bilzon, J., McCrory, P., 2011. Foot orthoses in the prevention of injury in initial military training: a randomized controlled trial. Am. J. Sports Med. 39, 30–37.

Gefen, A., 2003. Plantar soft tissue loading under the medial metatarsals in the standing diabetic foot. Med. Eng. Phys. 25, 491–499.

Gibson, K.S., Woodburn, J., Porter, D., Telfer, S., 2014. Functionally optimised orthoses for early rheumatoid arthritis foot disease: a study of mechanisms and patient experience. Arthritis Care Res. 66, 1456–1464.

Isvilanonda, V., Dengler, E., Iaquinto, J.M., Sangeorzan, B.J., Ledoux, W.R., 2012. Finite element analysis of the foot: model validation and comparison between two common treatments of the clawed hallux deformity. Clin. Biomech. 27, 837–844.

Mithraratne, K., Ho, H., Hunter, P.J., Fernandez, J.W., 2012. Mechanics of the foot Part 2: a coupled solid-fluid model to investigate blood transport in the pathologic foot. Int. J. Numer. Methods Biomed. Eng. 28, 1071–1081.

Oosterwaal, M., Telfer, S., Torholm, S., Carbes, S., van Rhijn, L.W., Macduff, R., Meijer, K., Woodburn, J., 2011. Generation of subject-specific, dynamic, multisegment ankle and foot models to improve orthotic design: a feasibility study. BMC Musculoskelet. Disord. 12, 256.

Owings, T.M., Woerner, J.L., Frampton, J.D., Cavanagh, P.R., Botek, G., 2008. Custom therapeutic insoles based on both foot shape and plantar pressure measurement provide enhanced pressure relief. Diabetes Care 31, 839–844.

Pai, S., Ledoux, W.R., 2010. The compressive mechanical properties of diabetic and non-diabetic plantar soft tissue. J. Biomech. 43, 1754–1760.
Petre, M., Erdemir, A., Panoskaltsis, V.P., Spirka, T.A., Cavanagh, P.R., 2013. Optimization of nonlinear hyperelastic coefficients for foot tissues using a magnetic resonance imaging deformation experiment. J. Biomech. Eng. 135, 61001–61012.
Petre, M.T., Erdemir, A., Cavanagh, P.R., 2006. Determination of elastomeric foam parameters for simulations of complex loading. Comput. Methods Biomech. Biomed. Eng. 9, 231–242.
R Development Core Team, 2014. R: A Language and Environment for Statistical Computing.
Spirka, T.A., Erdemir, A., Ewers Spaulding, S., Yamane, A., Telfer, S., Cavanagh, P.R., 2014. Simple finite element models for use in the design of therapeutic footwear. J. Biomech. 47, 2948–2955.
Tadepalli, S.C., Erdemir, A., Cavanagh, P.R., 2011. Comparison of hexahedral and tetrahedral elements in finite element analysis of the foot and footwear. J. Biomech. 44, 2337–2343.
Telfer, S., Woodburn, J., 2010. The use of 3D surface scanning for the measurement and assessment of the human foot. J. Foot Ankle Res. 3, 19.
Telfer, S., Erdemir, A., Woodburn, J., Cavanagh, P.R., 2014. What has finite element analysis taught us about diabetic foot disease and its management? A systematic review. PLoS One 9, e109994.
Ulbrecht, J.S., Hurley, T., Mauger, D.T., Cavanagh, P.R., 2014. Prevention of recurrent foot ulcers with plantar pressure-based in-shoe orthoses: the careful prevention multicenter randomized controlled trial. Diabetes Care 37, 1982–1989.
Wickham, H., 2009. ggplot2: Elegant Graphics for Data Analysis. Springer, New York.
Yavuz, M., Erdemir, A., Botek, G., Hirschman, G.B., Bardsley, L., Davis, B.L., 2007. Peak plantar pressure and shear locations: relevance to diabetic patients. Diabetes Care 30, 2643–2645.